Gas Phase Acidities of Organic Acids Based on 9H-Fluorene Scaffold: A DFT Study

Hamid Saeidian (saeidian1980@gmail.com)
Payame Noor University (PNU) https://orcid.org/0000-0003-1516-9178
Baharak Farzin
Islamic Azad University
Zohreh Mirjafary
Islamic Azad University

Research Article

Keywords: Superacid, DFT calculation, Aromaticity, MEP map, Deprotonation.

Posted Date: June 17th, 2021

DOI: https://doi.org/10.21203/rs.3.rs-605603/v1

Version of Record: A version of this preprint was published at Structural Chemistry on August 9th, 2021.
See the published version at https://doi.org/10.1007/s11224-021-01819-6.

Gas phase acidities of organic acids based on 9H-fluorene scaffold: A DFT Study

Hamid Saeidian,[*1] Baharak Farzin,[2] Zohreh Mirjafary[2]

[1] *Department of Science, Payame Noor University (PNU), P.O. Box: 19395-4697, Tehran, Iran*

[2] *Department of Chemistry, Science and Research Branch, Islamic Azad University, Tehran, Iran*

Email: Saeidian1980@gmail.com

Abstract: The density functional theory (DFT) calculations have been performed on a new set of organic Brønsted acids based on 9H-fluorene scaffold. The optimal structures and acidity of the compounds have been calculated by using DFT/B3LYP/6-31++G(d,p) computational method. The acidity of the designed compounds was obtained in the range of 276-328 kcal/mol that the fluorene scaffold bearing ketenimine group **17** and trifilic group **20** with ΔH_{acid} of 276.3 and 285.4 kcal/mol, respectively were found to be within the range of superacids, being more acidic than simple fluorene and mineral acids. The designed compounds and the corresponding conjugate bases were also examined from the aromaticity indices point of view. The tautomerization process for some designed structures was investigated by DFT calculations. Molecular electrostatic potential analysis for the designed acids and the corresponding conjugate bases were also used for charge distribution analysis.

Keywords: Superacid, DFT calculation, Aromaticity, MEP map, Deprotonation.

Introduction

Chemists have long regarded inorganic acids such as sulfuric, nitric, perchloric and hydrofluoric acids as the strongest available acidic systems. This perspective significantly changed with the discovery of systems with an acidity of 10^{12} times higher than sulfuric acid [1]. Hall and Conant

observed that weak organobases such as ketones and aldehydes could form salts with perchloric acid in nonaqueous solvents. Since perchloric acid can protonate such weak bases in nonaqueous systems, they called this acidic system as superacid [2]. Based on the researches of Gillespie *et al.*, who have carried out pioneering activities in the field of mineral aspects of the acidic systems, all protic acids stronger than 100% sulfuric acid should be classified as superacids [3]. Therefore, $HClO_4$, HSO_3F and CF_3SO_3H are referred to as superacids. A superacid can be protonated very weak bases such as methane, due to its very high acidity. The acidity threshold in the gas phase has been reported to be 300 kcal/mol [4]. Superacids and strong acids are used in cracking and alkylation processes and the chemical industry [5, 6]. The acidity of different acidic systems can be measured experimentally using UV-Vis and nuclear magnetic resonance spectroscopy [7, 8]. However, these experiments are typically performed in the solution phase, and the results are highly dependent on the properties of the solvent. In this regard, regardless of the type of solvent used, the gas phase acidity has been presented as a standard method for identifying the superacid properties. The gas phase acidity plays a significant role in the design of new superacids. Today, in computational chemistry, improving the acidity of organic compounds has attracted the attention of many researchers [9-18]. In most conducted studies, the negative charge on the corresponding conjugate base is stabilized by inductive effect, delocalization, and intramolecular hydrogen bonding.

The present research team has also conducted the DFT/B3LYP calculations on hybrid organic-inorganic acids to investigate their gas phase acidity [20-23]. A strong acidity value was predicted for a set of fluorosulfuric acids in which oxygen is replaced by an unsaturated ring [23]. The acidity of these acids without the electron withdrawing groups on the ring is greater than the fluorosulfuric

acid. It was observed that the replacement of hydrogen by electron withdrawing groups such as -CN and -F on the ring leads to an increment in the acidity up to the level of superacids.

Fluorene is a tricyclic aromatic hydrocarbon in which the five-membered ring has no aromaticity. The C9-H site of the fluorene ring has a weak acidity (pKa=22.6 in DMSO) whose protonation leads to forming of a stable aromatic anion with a bold orange color [24, 25]. According to the points mentioned above, and in continuation of previous works, the present study has attempted to design neutral organic superacids using fluorene scaffold and enole functional group and establish of substituents such as -F and -CN on the benzene rings (Scheme 1).

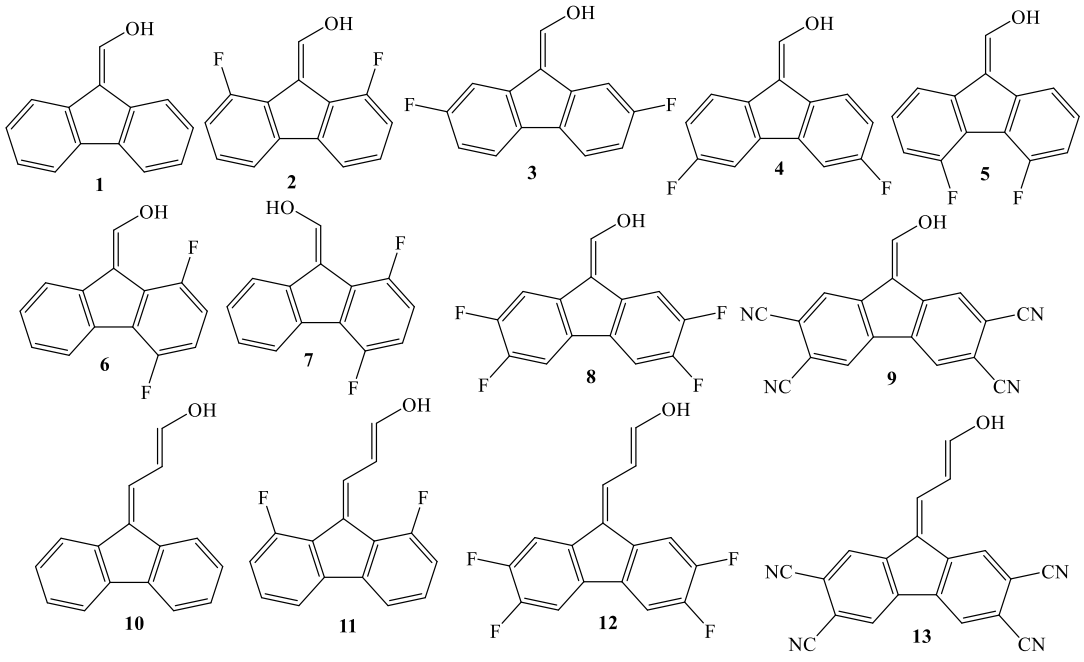

Scheme 1 The chemical structures of the proposed superacids bearing enole functional group.

In the second section of the study, other acidic functional groups were placed on the C9-H site of the fluorene ring to obtain hybrid organic-inorganic acids (Scheme 2).

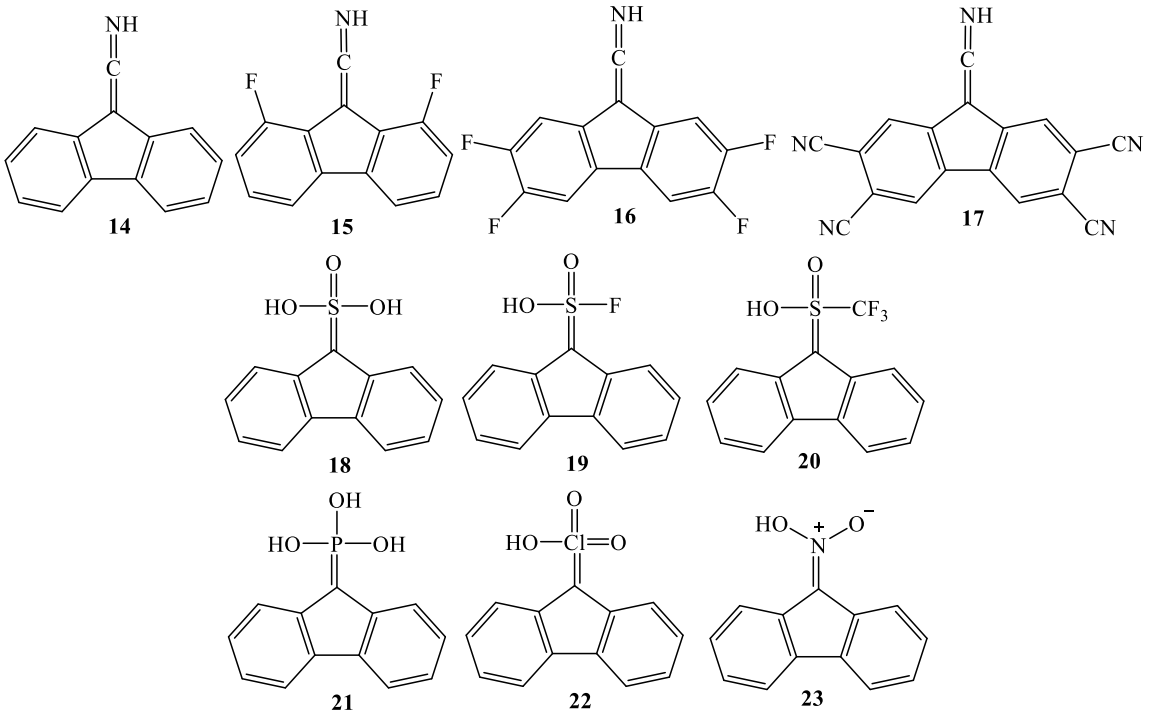

Scheme 2 The chemical structures of the proposed superacids bearing acidic functional groups.

Computational details

The geometric optimization and frequency calculations for all proposed structures have been carried out using Gaussian 09 software [26] and applying the DFT-B3LYP/6-31++G(d,p) computational method (Supporting Information). The frequency calculations were performed using the mentioned computational method to obtain the thermodynamic data of the deprotonation enthalpies (ΔH_{acid}) and Gibbs free energies (ΔG_{acid}) of the acids **1-23** (reaction 1) at 298 K (equations 1 and 2) [23]:

$$AH\ (g) \longrightarrow A^-\ (g) + H^+\ (g) \quad \textbf{(1)}$$

$$\Delta H_{acid} = H_{A^-} - H_{AH} + 1.48 \quad \textbf{(1)}$$

$$\Delta G_{acid} = G_{A^-} - G_{AH} - 6.27 \quad \textbf{(2)}$$

H_{AH}, H_{A^-}, G_{AH}, and G_{A^-} donate enthalpies and Gibbs free energies of the designed acid and its corresponding anions, respectively. For the proton, the following values were used: $H_{298}(H^+) = 1.48$ kJ mol^{-1} and $G_{298}(H^+) = -6.27$ kcal mol^{-1} [27, 28].

Results and discussion

Accuracy evaluation of computational method and the basis set used in the acidity estimation are of high prominence. Among the features of an ideal computational method, one can refer to the high computational speed and cost-effectiveness and increased accuracy in the computational methods. It is saying that the DFT/B3LYP method usually leads to accurate results regarding the physicochemical properties of organic compounds such as protonation and deprotonation processes [29-31]. To find an accurate and computationally efficient method, the two computational B3LYP and MP2 methods have been compared in this study. For this purpose, the bond lengths and ΔH_{acid} associated with compound **1** have been calculated using the above two computational methods and the results are presented in Table 1.

Table 1 Calculated bond lengths and ΔH_{acid} of **1** by using the DFT/ B3LYP and MP2 methods with 6-31++G(d,p) basis set.

Molecule	bond lengths (Å)	Calculated method		calculated ΔH_{acid} (kcal/mol)	
		B3LYP	MP2	B3LYP	MP2
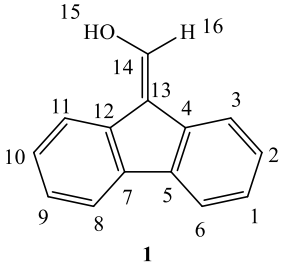 **1**	C^{14}- H^{16}	1.087	1.085	323.0	321.9
	C^{14}- O^{15}	1.346	1.369		
	C^{13}- C^{14}	1.347	1.352		
	C^{12}- C^{13}	1.473	1.467		
	C^{12}- C^{7}	1.420	1.419		

C^{11}- C^{12}	1.398	1.401

As would be observed, there is a relatively good agreement between the two methods. The plot of the calculated bond lengths obtained from the DFT method *vs* the calculated data from MP2 indicates a linear relationship with a regression value of $r^2 = 0.994$, as shown in Fig. 1.

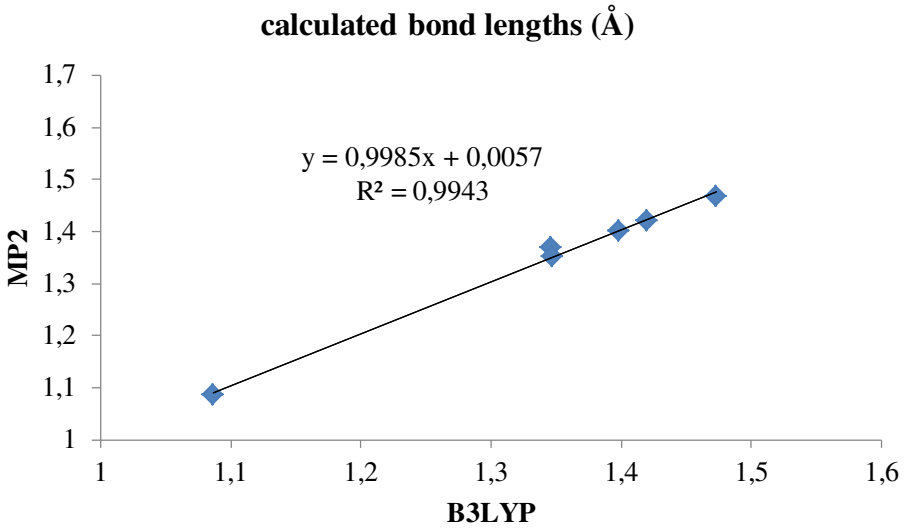

Fig. 1 The linear regression between B3LYP calculated bond lengths and MP2 methods for **1**.

The acidity of **1** was also calculated using the two mentioned methods, and the results showed that the enthalpy values were almost the same (Table 1). Therefore, the B3LYP/6-31++G(d, p) method is expected to be suitable for calculating the ΔH_{acid} of the designed acids **1-23**.

The prototropic tautomers of the chemicals **1**, **14** and **18** were shown in Scheme 3 with their relative energies in kcal/mol. The C-H tautomers are more stable than the proposed structures in Scheme 1

and 2. In the present study, the structures in Scheme 1 and 2 were considered and their ΔH_{acid} were calculated by DFT calculations.

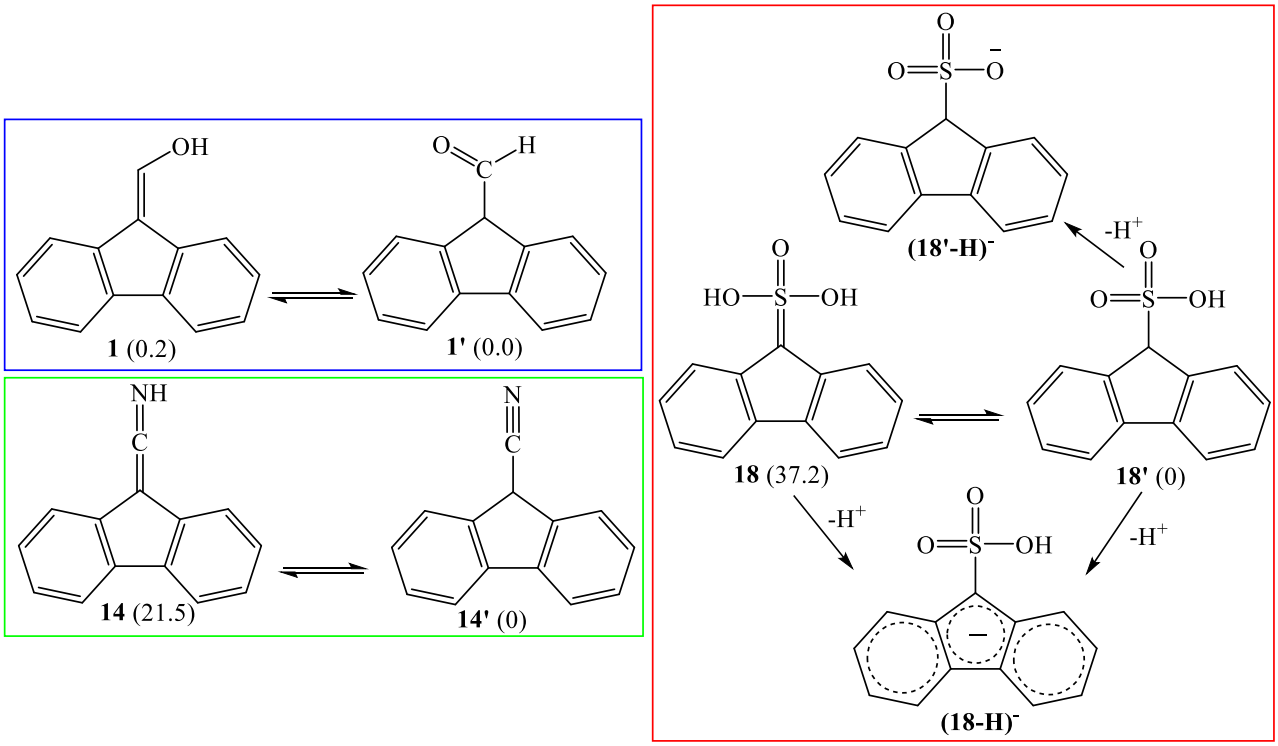

Scheme 3 Tautomerization of **1, 14, 18** and their relative energies in kcal/mol.

Some optimized structures of the examined compounds **1-23** at the B3LYP/6-31++G(d,p) computational level are shown in Fig. 2.

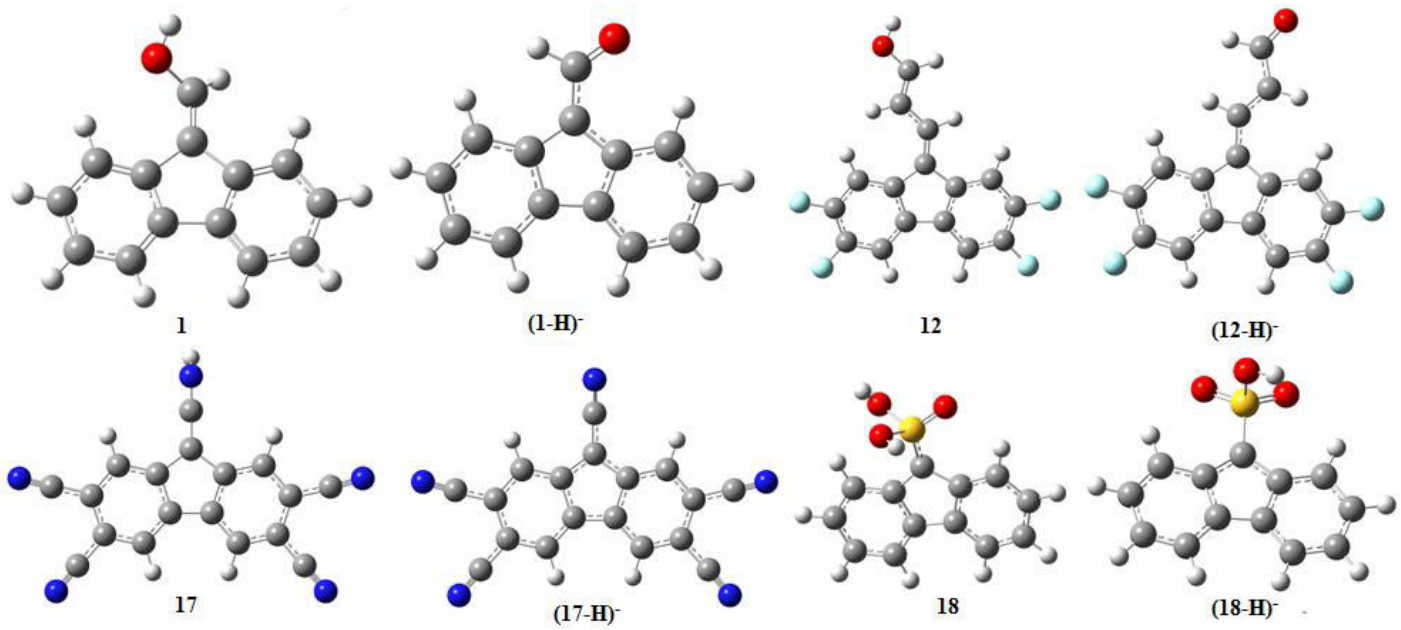

Fig. 2 Some optimized structures of **1-23** and their corresponding conjugate bases at the B3LYP/6-31++G(d,p).

Usually, the strong acid is related to the more stable the resultant conjugate base (anion). Upon deprotonating the designed acids **1-23**, the negative charge is expected to be delocalized over the rings and reach stability. According to the Hückel's rule, placing of a negative charge on the cyclopentadiene ring in fluorene framework leads to its aromatization (Scheme 4). Therefore, the evaluation of aromaticity indices in corresponding conjugate bases is so essential. Aromaticity cannot be experimentally measured. Aromaticity is a phenomenon that can be described by different descriptors such as structural, energy and magnetic properties.

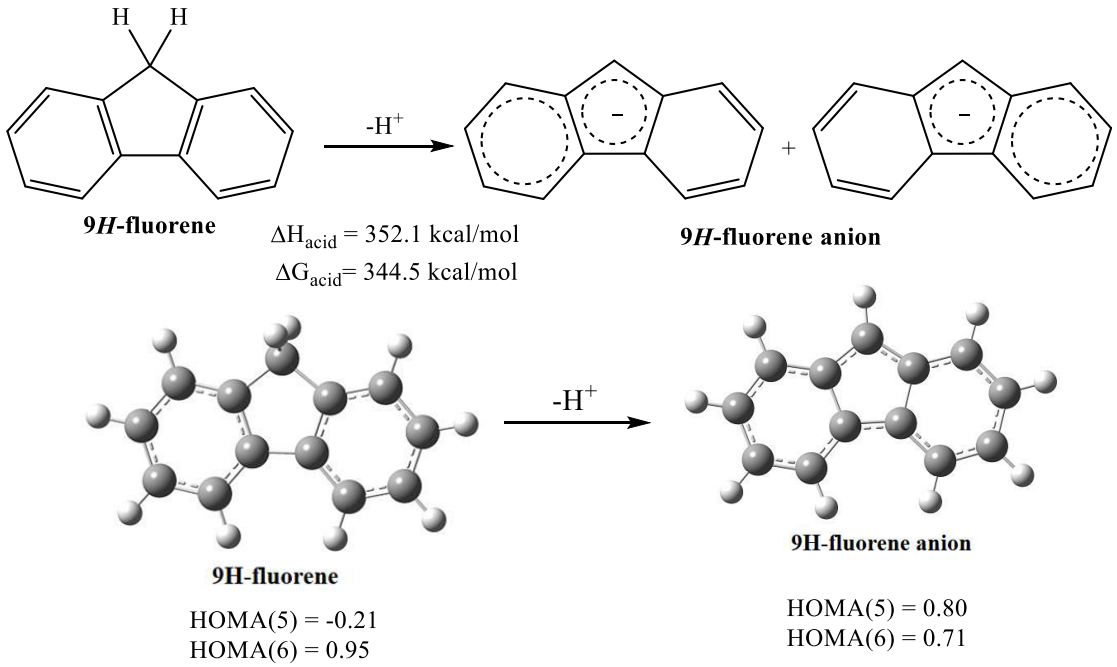

Scheme 4 Deprotonation of 9H-fluorene results an aromatic system.

The nucleus-independent chemical shift (NICS) [32] and harmonic oscillator model of aromaticity (HOMA) [33] are among the efficient methods for determining the aromaticity of cyclic compounds. The NICS parameter is calculated as the negative magnetic charge shielding at intervals in the center, top and bottom of the ring. The NICS measurement at a distance of 1 Å above the ring using GIAO method [34] and bq dummy atom as a probe has been reported to be the best way to accurately determine the aromaticity characteristics. The negative and positive NICS values indicate the aromaticity and antiaromaticity natures of the examined compounds, respectively. HOMA index is a geometric descriptor of aromaticity based on the bond length. This index is calculated for homoaromatics by using equation (3) [35].

$$\mathrm{HOMA} = 1 - \frac{\alpha}{n} \sum_{i=1}^{n} \left(R_i - R_{opt}\right)^2 \qquad (3)$$

Here, n indicates the number of carbon atoms in the ring under study, and the normalization factor α is 257.7. In equation (3), R_i and R_{opt} stand for the length of C-C bonds in the investigated

aromatic ring and an ideal aromatic system such as benzene, respectively. Krygowski reported the d_{opt} value as equal to 1.388 Å for benzene [33]. On the other hand, the B3LYP/6-311+G(d,p) calculated R_{opt} for ionic homoaromatic $C_5H_5^-$ is 1.415 [36]. It should be noted that HOMA is equal to 1 for the benzene ring, and the aromaticity of other compounds are compared with this value. The HOMA and NCIS values were calculated and reported for the studied compounds. Table 2 and 3 present the values of ΔH_{acid}, ΔG_{acid}, HOMA and NICS associated with compounds **1-23** and their anions.

Table 2 The calculated ΔH_{acid}, ΔG_{acid}, HOMA and NICS data for acids **1-13**.

Compound	ΔH_{acid}[a]	ΔG_{acid}[a]	NICS(1)[b]	HOMA
Fluorene	352.1	344.5	-1.87	0.21(0.95)[c]
(Fluorine-H)$^-$	-	-	-12.80	0.80(0.71)[c]
1	323.0	315.7	-2.30	0.45(0.93)[c]
(1+H)$^-$	-	-	-8.95	0.78(0.85)[c]
1´	323.3	316.7	-1.03	0.29(0.95)[c]
(1´+H)$^-$	-	-	-8.95	0.78(0.85)[c]
2	328.2	319.9	-3.16	0.49(0.93)[c]
(2+H)$^-$	-	-	-9.38	0.77(0.76)[c]
3	316.3	308.9	-2.25	0.49(0.94)[c]

(3+H)$^-$	-	-	-8.42	0.83(0.84)[c]
4	318.2	310.8	-2.63	0.50(0.94)[c]
(4+H)$^-$	-	-	-9.24	0.80(0.86)[c]
5	316.5	309.1	-2.54	0.50(0.93)[c]
(5+H)$^-$	-	-	-8.89	0.78(0.83)[c]
6	325.9	317.7	-2.62	0.51 (0.93)[c] (0.84)[d]
(6+H)$^-$	-	-	-11.76	0.80 (0.85)[c] (0.83)[d]
7	319.0	311.5	-2.62	0.54 (0.93)[c] (0.95)[d]
(7+H)$^-$	-	-	-8.82	0.80(0.85)[c] (0.83)[d]
8	312.0	304.6	-2.56	0.51 (0.95)[c]
(8+H)$^-$	-	-	-8.98	0.81(0.86)[c]
9	287.2	279.9	-3.91	0.46 (0.89)[c]
(9+H)$^-$	-	-	-10.10	0.85 (0.77)[c]
10	317.7	310.8	-1.97	0.43(0.94)[c]

(10+H)$^-$	-	-	-7.69	0.74(0.85)[c]
11	316.9	309.5	-2.91	0.44(0.95)[c]
(11+H)$^-$	-	-	-8.76	0.74(0.86)[c]
12	308.8	301.6	-2.31	0.47(0.96)[c]
(12+H)$^-$	-	-	-8.11	0.77(0.86)[c]
13	287.3	280.0	-3.98	0.56(0.87)[c]
(13+H)$^-$	-	-	-9.71	0.83(0.75)[c]

[a] B3LYP/6-31++G(d,p), kcal/mol, at 298 K; [b] Calculated at GIAO-B3LYP/6-31++G(d, p) level and in ppm; [c] For 6-membered ring; [d] For 6-membered ring bearing fluorine atoms

As mentioned above, the 9H-fluorene molecule is a weak acid. According to Scheme 4, this compound is converted to a stable anion by losing a proton. The HOMA and NICS values have been calculated for the five- and six-membered fluorene rings (Table 2). According to the estimated values, it can be observed that the five-membered ring is not aromatic in neutral form. Due to deprotonation, the HOMA and NICS values in the anionic form have significantly increased, indicating the aromatization of the five-membered ring and negative charge stability as well. It is also worth noting that the aromaticity indices of benzene rings in the anionic form are expected to decrease relative to the neutral one. The resonance energy of the molecule in the anionic form is distributed between all the rings. In contrast, in the neutral form two separate benzene rings have their own energy. Comparing the aromaticity indices in the neutral and anionic forms of all studied compounds testifies to this point (Table 2 and 3). Adding an enole group to the C9-H of the fluorene ring results in acid **1** with an acidity of ΔH_{acid} = 323.0 kcal/mol, which is more acidity than

simple 9H-fluorene to amount of 29.1 kcal/mol. Placing fluorine atoms on the aromatic rings in different situations leads to compounds **2-8**. Compound **2** bearing two electronegative fluorine atoms on C1 and C8 has ΔH_{acid} = 328.2 kcal/mol while the acidity of **3** with two –F on C2 and C7 is ΔH_{acid} = 316.3 kcal/mol. Among the acids **2-8**, compound **3** is the strongest superacid which may be due to the proper symmetry of the compound and appropriate delocalization of the negative charge in its corresponding conjugate base. Replacing hydrogen on C3 and C6 with fluorine atoms at 9H-fluorene structure resulted in compound **4** with ΔH_{acid} = 318.2 kcal/mol that is 33.9 kcal/mol lower than 9H-fluorene. According to the data in Table 2, it is clear that compound **5** bearing fluorine atoms meet one of the highest acidities (ΔH_{acid} = 316.5 kcal/mol). The fluorine electron-withdrawing substituents are positioned in this compound in such a way that they meet maximum repulsion concerning to each other (Fig. 3). Therefore, compound **5** is unstable and deprotonation has caused the aromaticity parameters of the five-membered ring to be significantly increased in the conjugate base of **5** and stabilized as well. Stability of the conjugate base **(5-H)**$^-$ due to the increased aromaticity leads to an improvement in the acidity of compound **5**.

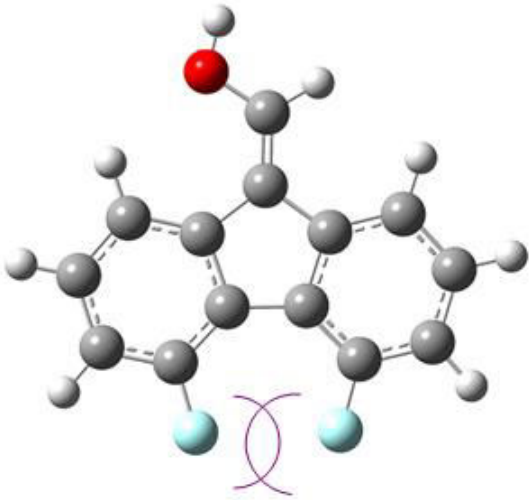

5

Fig. 3 Repulsion between two fluorine atoms in structure of **5**.

Moreover, simultaneous placement of two fluorine atoms on a benzene ring in acid **6** has been investigated. It is observed that the acidity of this compound has increased compared to **2**, however it is lower than that of compounds **3-5**. It should be noted that molecules **2** and **6** are relatively stable due to the formation of intramolecular hydrogen bonding between the -F and the -OH group and do not tend to lose proton (Fig. 4).

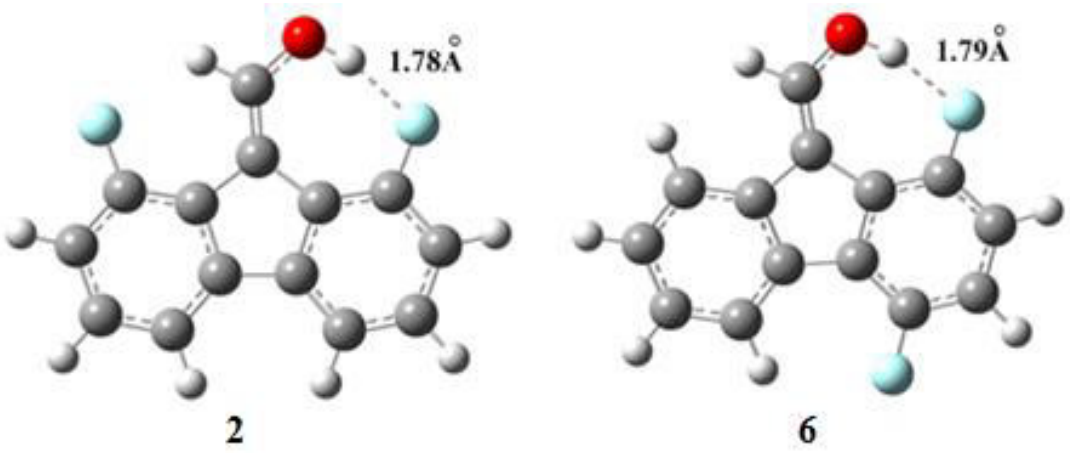

Fig. 4 Strong intramolecular hydrogen bonding in the structures of **2** and **6**.

Compound **6** has an asymmetric structure and the negative charge distribution is not uniform in it. Examination of HOMA indices in the three rings of five-membered one, benzene and benzene ring containing two -F atoms, shows that the stability of the five-membered ring has dramatically increased, while no significant change can be observed in the stability of the benzene rings. The negative charge in this molecule has a greater tendency to form resonance in the five-membered ring, and therefore the HOMA index significantly increases. Compound **6** and **7** are geometrical isomers to each other, ***Z*-6** and ***E*-7**. It was found that the formation of intramolecular hydrogen bonding between the -F atom and the -OH group in the ***Z*-6** isomer leads to a reduction in the acidity by about 6-7 kcal mol^{-1}. We carried out a computational investigation on structure **8** bearing four F atoms. Using four F atoms on benzene rings results in acidity enhancement to 312.0 kcal/mol

for **8**. The fluorine atom is a strong electron-withdrawing group while having a low electron acceptor tendency due to its small atomic radius. The cyano group is an appropriate electron acceptor group. It needs less steric requirements for delocalization of negative charge of the corresponding conjugate base. The -CN groups can easily delocalize negative charge with resonance and inductive effect and increase the stability and consequently improve the acidity of the examined compounds and achieve strong acids. According to Table 2, it can be observed that the acidity of compound **9** has significantly increased by adding four cyano groups being higher than that of **1** to the amount of 36 kcal mol^{-1}. B3LYP/6-31++G(d,p) calculations reveal that compound **9** exhibits strong acidity to superacid behavior, ΔH_{acid} = 287.2 kcal/mol. The HOMA index in the conjugate base of **9** has increased by about 0.39, which increases the aromaticity of the five-membered ring and improves its acidity as a consequence.

The π system expansion usually results in better delocalization of negative charge throughout the molecule. Hence, a double bond was added to the enole structure of compound **1**. Contrary to expectations, a decrease in ΔH_{acid} was observed. However, adding four -CN electron-withdrawing groups to **10** has led to the formation of structure **13**, whose acidity has been estimated to be higher than that of the basic fluorene molecule to the amount of 65 kcal mol^{-1} and falls within the range of superacids [4].

The findings prompted us to investigate new superacids based on the strong inorganic acids of perchloric, sulfonic, nitric and phosphoric acid (Table 3). Furthermore, the effect of adding C=C=NH substituent was investigated on the acidity of **14-17**. According to Table 3, it can be seen that adding the ketenimine group (-C=C=NH) has led to an increment in the acidity of compound **14** to the amount of 302.9 kcal mol^{-1}, which can be classified as a strong N-H acid. This significant increase in acidity is mainly due to the expansion of the π-conjugate system, which stabilizes the

corresponding anion and thus improves its acidity. Also, the NICS index of the five-membered ring has drastically increased (-10.85 ppm) as well as the HOMA index (0.83), which indicates the importance of this ring in stabilizing the negative charge in the anion **(14-H)**$^-$.

Table 3 The calculated ΔH_{acid}, ΔG_{acid}, HOMA and NICS data for acids **14-23**.

Compound	ΔH_{acid}[a]	ΔG_{acid}[a]	NICS(1)[b]	HOMA
14	302.9	295.5	-5.61	0.61(0.92)[c]
(14+H)$^-$	-	-	-10.85	0.83(0.82)[c]
14´	325.8	317.0	-3.20	0.50(0.96)[c]
(14´+H)$^-$	-	-	-10.85	0.83(0.82)[c]
15	311.6	304.0	-4.21	0.57(0.94)[c]
(15+H)$^-$	-	-	-11.04	0.85(0.82)[c]
16	303.0	294.5	-3.92	0.53(0.95)[c]
(16+H)$^-$	-	-	-10.71	0.85(0.96)[c]
17	276.3	268.9	-5.18	0.61(0.88)[c]
(17+H)$^-$	-	-	-11.27	0.87(0.75)[c]
18	291.9	285.0	-4.91	0.92(0.57)[c]
(18+H)$^-$	-	-	-10.26	0.82(0.84)[c]

18´	313.0	305.9	-2.26	0.21(0.95)[c]
(18´+H)$^-$	-	-	-10.26	0.82(0.84)[c]
19	286.8	279.8	-3.03	0.51(0.93)[c]
(19+H)$^-$	-	-	-8.25	0.78(0.82)[c]
20	285.4	278.5	-5.14	0.53(0.93)[c]
(20+H)$^-$	-	-	-9.52	0.78(0.86)[c]
21	303.9	296.4	-6.74	0.62(0.90)[c]
(21+H)$^-$	-	-	-10.11	0.81(0.82)[c]
22	305.5	300.8	-1.34	0.64(0.92)[c]
(22+H)$^-$	-	-	-10.33	0.75(0.83)[c]
23	317.9	310.7	-1.63	0.58(0.93)[c]
(23+H)$^-$	-	-	-6.88	0.79(0.87)

[a] B3LYP/6-31++G(d,p), kcal/mol, at 298 K; [b] Calculated at GIAO-B3LYP/6-31++G(d, p) level and in ppm; [c] For 6-membered ring

In addition, the effects of four cyano groups on the acidity of compound **14** were also investigated. The remarkable stability of compound **17** with ΔH_{acid} = 276.3 kcal/mol indicated that this compound is the strongest superacid among the examined structures. Among the studied hybrid organic-inorganic acids **18-23**, it can be clearly observed that the acidity of the compounds based on sulfuric acid **18-20** has remarkably increased and the strongest superacids have been obtained with

acidity in the range of 285.4-291.9 kcal/mol. All the proposed acids **18-20** are more acidic than H_2SO_4 (ΔH_{acid} = 311.5 kcal/mol) and FSO_3H (ΔH_{acid} = 301.3 kcal/mol) [37]. Superacid **20** based on trifluoromethane sulfonic acid (trifilic acid) meet the high acidity 285.4 kcal/mol. This can be attributed to the electron-withdrawing group of $-CF_3$, which has well improved the stability of the negative charge in the conjugate base. It is also observed that adding of fluorine atom instead of the hydroxyl group in the sulfuric acid-based superacid **18** (compound **19**) has led to a slight increase in the acidity compared to compound **18** by about 5.5 kcal mol^{-1}. Fig. 5 shows a comparison between the bond lengths in **19** and its corresponding conjugate base **(19-H)**$^-$. As would be observed, due to the negative charge stability in the conjugate base of **19**, the bond lengths have increased in the five-membered ring, which indicates the presence of resonance phenomena in anion structure **(19-H)**$^-$.

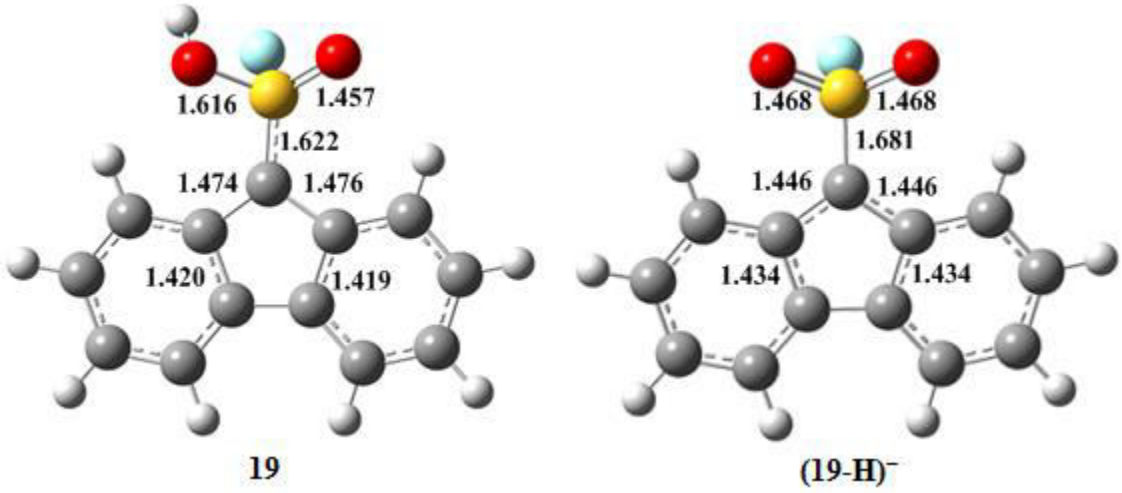

Fig. 5 The optimized structures of **19** and **(19-H)**$^-$. The bond distances are in (Å).

Finally, it was claimed that for the conjugate bases of **1-23**, the negative charge is placed on the cyclopentadiene ring. Molecular electrostatic potential (MEP) maps can also be used to support this claim [38]. The MEP map provides the charge distributions of molecules in three-dimensional

space, the positive (blue) and negative (red). Calculated acidities at B3LYP/6-31++G(d, p) level are the highest for molecules **17** and **20**. Therefore as representative examples, MEP maps of **17**, **20** and the corresponding conjugate bases are shown in Fig. 6. As would be observed, the negative charge in **(17-H)**$^-$ and **(20-H)**$^-$ is placed on the five-membered ring. Some common features can be observed in the MEP maps. The positive charge (blue region) is mainly localized on the hydrogen atom of the acid unit and this will favor deprotonation.

The regions governing the electron-rich nitrile groups in **(17-H)**$^-$ are strongly negative (red color), which confirms the high capacity of –CN group for delocalization of negative charge. It can be seen from MEP of **(20-H)**$^-$ that the negative charge is distributed throughout the structure.

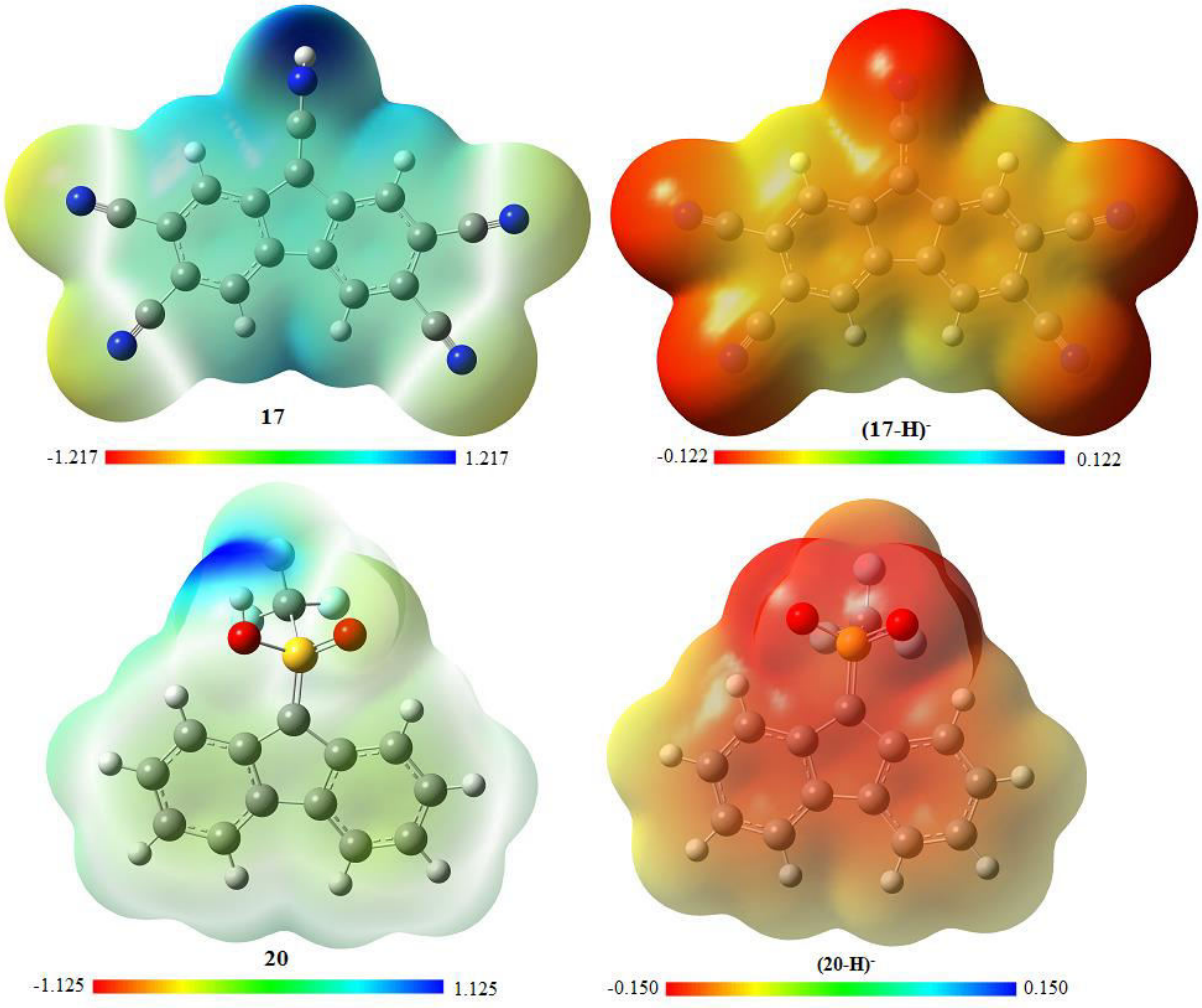

Fig. 6 Molecular electrostatic potential surface for acid **17** and **20,** as well as their conjugate bases.

Conclusion

A new category of organic fluorene acids (23 structures) was designed and their acidities were investigated by DFT/B3LYP/6-31++G(d, p) method. Some designed structures are more acidic than fluorene and even inorganic acids such as H_2SO_4 and FSO_3H. Upon deprotonation, the negative charge is delocalized in the cyclic framework, which led to an aromatic system. This is in harmony with aromatic indices (NICS and HOMA) and MEP analysis of the corresponding conjugate base of acids. Substitution of electron-withdrawing groups, -CN and -F on cyclic framework enhanced the acidity. The ΔH_{acid} values were calculated in the range of 276.2-328.2 kcal/mol, which some fall into the defined range of superacidity.

Declaration

Funding

Not applicable

Conflict of interest

The authors declare that they have no conflict of interest

Availability of data and material

The online version of this article contains supplementary material, which is available to authorized users.

Code availability

Not applicable.

Authors' contributions

Hamid Saeidian: Conceptualization, Formal analysis, Investigation, Resources, Software, Validation, Visualization, Writing- review & editing. **Baharak Farzin:** Formal analysis, Investigation, Resources,

Software, Validation, Visualization. **Zohreh Mirjafary:** Conceptualization, Formal analysis, Investigation, Resources, Software, Validation, Visualization, Writing- review & editing.

References

1. Olah GA, Prakash GS, Sommer J, Molnar A (2009). Superacid Chemistry. John Wiley & Sons Inc.
2. Hall NF, Conant JB (1927). J Am Chem Soc 49:3062-3070.
3. Gillespie RJ, Peel TE, Robinson EA (1971). J Am Chem Soc 93:5083-5087.
4. Vianello R, Maksić ZB (2008). New J Chem 32:413-427.
5. Greb L (2018). Chem A Eur J 24:17881-17896.
6. Prakash GS, George A, Olah GK, Prakash (2004). Organic Synthesis in Superacids, in Carbocation Chemistry. John Wiley & Sons Inc.
7. Pagni RM. (2009). Found Chem 11:43-50.
8. Yang W, Wang Z, Huang J , Jiang Y (2021) J Phys Chem C 125:10179–10197.
9. Raczyńska ED, Gal JF, Maria PC (2016). Chem Rev 116:13454-511.
10. Koppel IA, Taft RW, Anvia F, Zhu SZ, Hu LQ, Sung KS, DesMarteau DD, Yagupolskii LM, Yagupolskii YL (1994). J Am Chem Soc 116:3047-3057.
11. Yáñez M, Mó O, Alkorta I, Elguero J (2013). Chem A Eur J 19:11637-11643.
12. Rasheed T, Siddiqui SA, Kargeti A, Shukla DV, Singh V, Pandey AK (2021). https://doi.org/10.1007/s11224-021-01786-y.
13. Lipping L, Leito I, Koppel I, Krossing I, Himmel D, Koppel IA (2015). J Phys Chem A 119:735-743.
14. Vianello R, Maksić ZB (2009). New J Chem 33:739-48.
15. Alcami M, Mo O, Yanez M (2002). J phys Org Chem 15:174-186.
16. Si MK, Ganguly B (2017). New J Chem 41:1425-1429.

17. Vianello R, Liebman JF, Maksić ZB (2004). Chem A Eur J 10:5751-5760.

18. Srivastava AK, Kumar A, Misra N (2017). J Fluor Chem 197:59-62.

19. Rocha AS, Costa GC, Tamiasso-Martinhon P, Sousa C, Rocha AB (2017). Mater Chem Phys 186:138-145.

20. Saeidian H (2020). Struct Chem 31:851-859.

21. Saeidian H, Mashhadian S, Mirjafary Z, Rouhani M (2019). Comput Theor Chem 1157:11-18.

22. Saeidian H, Shams B, Mirjafary Z (2019). Struct Chem 30:787-793.

23. Shams B, Saeidian H (2018). Comput Theor Chem 1135:48-55.

24. Bordwell FG (1988). Acc Chem Res 21: 456–463.

25. Scherf GW, Brown RK (1960). Can J Chem 38:697-712.

26. Frisch MJ, Trucks GW, Schlegel HB, Scuseria GE, Robb MA, Cheeseman JR, Zakrzewski VG, Montgomery JA, Jr Stratmann RE, Burant JC, Dapprich S, Millam JM, Daniels AD, Kudin KN, Strain MC, Farkas O, Tomasi J, Barone V, Cossi M, Cammi R, Mennucci B, Pomelli C, Adamo C, Clifford S, Ochterski J, Petersson GA, Ayala PY, Cui Q, Morokuma K, Salvador P, Dannenberg JJ, Malick DK, Rabuck AD, Raghavachari K, Foresman JB, Cioslowski J, Ortiz JV, Baboul AG, Stefanov BB, Liu G, Liashenko A, Piskorz P, Komaromi I, Gomperts R, Martin RI, Fox DJ, Keith T, Al-Laham MA, Peng CY, Nanayakkara A, Challacombe M, Gill PMW, Johnson BG, Chen W, Wong MW, Andres JL, Gonzalez C, Head-Gordon M, Replogle ES, Pople JA (2013) Gaussian 09, Gaussian, Inc. Wallingford CT.

27. Bartmess JE (1994). J Phys Chem 98:6420-6424.

28. Krygowski TM (1993). J Chem Inf Comput Sci 33:70-78.

29. Bryantsev VS, Diallo MS, Van Duin AC, Goddard WA (2009). J Chem Theory Comput 5:1016-1026.

30. Singh A, Ojha AK, Jang HM (2018). ChemistrySelect3:837-842.

31. Geerlings P, De Proft F, Langenaeker W (2003). Chem Rev 103:1793-1874.

32. Chen Z, Wannere CS, Corminboeuf C, Puchta R, Schleyer PV (2005).

33. Chem Rev 101:1385-1420.

34. Wolinski K, Hinton JF, Pulay P (1990). J Am Chem Soc 112:8251-8260.

35. Krygowski TM, Szatylowicz H, Stasyuk OA, Dominikowska J, Palusiak M (2014). Chem Rev 114:6383-422.

36. Raczyńska ED, Hallman M, Kolczyńska K, Stępniewski TM (2010). Symmetry 2:1485-1509.

37. Koppel IA, Burk P, Koppel I, Leito I, Sonoda T, Mishima M (2000). J Am Chem Soc 122:5114-5124.

38. Tasi G, Palinko I (1995). Using molecular electrostatic potential maps for similarity studies, in Molecular Similarity II. Topics in Current Chemistry, (Ed: K. D. Sen) Vol. 174, Springer, Berlin, Heidelberg.

Supplementary Files

This is a list of supplementary files associated with this preprint. Click to download.

- GraphicalAbstract.doc
- ESI.docx